Available online www.jocpr.com

Journal of Chemical and Pharmaceutical Research, 2013, 5(12):1474-1481

Research Article

ISSN : 0975-7384
CODEN(USA) : JCPRC5

Gravimetric and electrochemical impedance spectroscopy study for 4-(2-chlorobenzyl)-6-hydrazino-3-methyl-1,6-dihydropyridazine as inhibitor corrosion for copper in nitric acid

L. Afrine[1], A. Zarrouk[2], H. Zarrok[3], R. Salghi[4], R. Touir[5], B. Hammouti[2], H. Oudda[3], M. Assouag[3], H. Hannache[1], M. El Harti[1] and M. Bouachrine[6]

[1]*Laboratoire d'Ingénierie et Matériaux: Equipe des Matériaux Thermo-Structuraux et Polymères, Université Hassan II-Mohammedia, Faculté des Sciences Ben M'Sik, Casablanca, Maroc*
[2]*LCAE-URAC 18, Faculty of Science, University of Mohammed Premier, Oujda, Morocco*
[3]*Laboratory Separation Processes, Faculty of Science, University Ibn Tofail, Kenitra, Morocco*
[4]*Laboratory of Environmental Engineering and Biotechnology, ENSA, University Ibn Zohr, Agadir, Morocco*
[5]*Materials, Electrochemical and Environment Laboratory, Faculty of Science, University Ibn Tofail, Kenitra, Morocco*
[6]*ESTM, Université Moualy Ismail, Meknes, Morocco*

ABSTRACT

Corrosion inhibition effect of 4-(2-chlorobenzyl)-6-hydrazino-3-methyl-1,6-dihydropyridazine (P2) on copper corrosion was studied in 2.0 M HNO_3 solutions in the temperature range from 303K to 343K using gravimetric and electrochemical impedance spectroscopy (EIS) technique. The results obtained from the both measurement techniques revealed good inhibitor efficiency in the studied concentration range. The inhibition efficiency decrease with rise in temperature. Impedance measurements showed that the double-layer capacitance decreased and charge-transfer resistance increased with increase in the inhibitor concentration and hence increasing in inhibition efficiency. The results obtained from the different methods are in good agreement. Various parameters (E_a, ΔG_{ads}, K_{ads}) for adsorption reveal a strong interaction between inhibitor and copper surface. Adsorption followed the Langmuir isotherm with negative values of ΔG_{ads} , suggesting a stable and a spontaneous inhibition process. Kinetic parameters activation such as E_a, ΔH_a, ΔS_a and pre-exponential factor have been calculated and discussed.

Keywords: Pyridazine inhibitor, Copper, HNO_3, EIS, Gravimetric.

INTRODUCTION

The chemical industry employs copper and its alloys extensively for condensers, evaporators, fractionating columns, etc. Copper does not displace hydrogen from acid solutions and it is therefore unattacked in non-oxidising acid environments. Nevertheless, most acidic solutions contain dissolved air that enables some corrosion to take place. Acid solutions are commonly used for removal of undesirable scale and rust in the metal working, cleaning of boilers, heat exchangers, etc. [1-4]. In recent years, the use of organic inhibitors in acidic media has gained popularity. It has been shown that organic compounds containing heteroatoms with high electron density such as phosphor, nitrogen, sulphur, oxygen as well as those containing multiple bonds which are considered as adsorption centers, are effective as a corrosion inhibitor [5-28].

It is accepted that the organic inhibitors act by adsorption on the metal surface. The adsorption of organic inhibitors on the metal surface can change the corrosion resisting properties of the metals. The adsorption ability of these molecules depends mainly on certain physicochemical properties of the inhibitor molecule such as functional

groups, steric factor, aromaticity, electron density at the donor atoms and π orbital character of donating electrons and electronic structure of the molecule. Inhibitors behave as a protective barrier against the attack of the corrosive environment and can provide protection for the metal and so, they reduce corrosion rate of the metal.

This paper reported our attempt to use electrochemical impedance spectroscopy (EIS) and weight loss to investigate the nature of adsorption of pyridazine on the copper surface. The chemical structure of the studied P2 derivative is given in Fig 1.

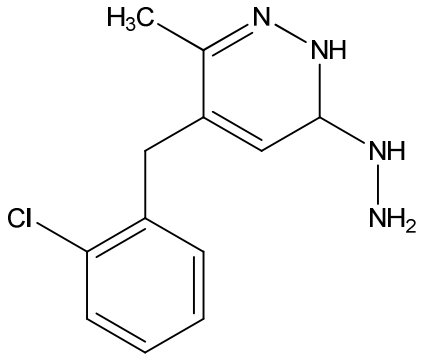

Figure 1. The chemical structure of the studied pyridazine derivative compound

EXPERIMENTAL SECTION

Materials and reagents

Copper strips containing 99.5 wt.% Cu, 0.001wt.% Ni, 0.019 wt.% Al, 0.004 wt.% Mn, 0.116 wt.% Si and balance impurities were used for electrochemical and gravimetric studies. The copper samples were mechanically polished using different grades of emery paper, washed with double distilled water, and dried at room temperature. Appropriate concentration of aggressive solutions used (2.0 M HNO_3) was prepared using double distilled water.

Weight loss measurements

Gravimetric experiments were carried out in a double walled glass cell. The solution volume was 50 cm^3; the temperature of 303 K was controlled thermostatically. The weight loss of copper in 2.0 M HNO_3 with and without the addition of inhibitor was determined after immersion in acid for 1 h. The copper specimens were rectangular in the form (2 cm ×2 cm × 0.20 cm).

Electrochemical impedance spectroscopy

The electrochemical measurements were carried out using Volta lab (Tacussel- Radiometer PGZ 301) potentiostate and controlled by Tacussel corrosion analysis software model (Voltamaster 4) at under static condition. The corrosion cell used had three electrodes. The reference electrode was a saturated calomel electrode (SCE). A platinum electrode was used as auxiliary electrode of surface area of 1 cm^2. The working electrode was copper. All potentials given in this study were referred to this reference electrode. The working electrode was immersed in test solution for 30 minutes to a establish steady state open circuit potential (*E*ocp). After measuring the *E*ocp, the electrochemical measurements were performed. All electrochemical tests have been performed in aerated solutions at 303 K. The EIS experiments were conducted in the frequency range with high limit of 100 kHz and different low limit 0.1 Hz at open circuit potential, with 10 points per decade, at the rest potential, after 30 min of acid immersion, by applying 10 mV ac voltage peak-to-peak. Nyquist plots were made from these experiments. The best semicircle can be fit through the data points in the Nyquist plot using a non-linear least square fit so as to give the intersections with the *x*-axis.

RESULTS AND DISCUSSION

Electrchemical Impedance Spectroscopy (EIS)

Nyquist plots of Corrosion inhibition effect of 4-(2-chlorobenzyl)-6-hydrazino-3-methyl-1,6-dihydropyridazine (P2) compound in 2.0 M HNO_3 solutions in the absence and presence of various concentrations of P2 is given in Fig 2. The impedance spectra show that a single semicircle and the diameter of semicircle increases with increasing inhibitor concentration. These diagrams exhibit that the impedance spectra consist of one capacitive loop at high frequency, the high frequency capacitive loop was attributed to charge transfer of the corrosion process [29]. The depressed form of the higher frequency loop reflects the surface inhomogeneity of structural or interfacial origin, such as those found in adsorption processes [30]. Various parameters such as charge-transfer resistance (R_{ct}), double layer capacitance (C_{dl}), f_{max} and inhibition efficiency were obtained from impedance measurements and are shown in

Table 1. R_{ct} values were calculated from the difference in impedance at lower and higher frequencies as suggested by Tsuru et al. [31]. C_{dl} values were calculated from the frequency at which the imaginary component of impedance was maximum (Z_{im} max) using the reaction:

$$C_{dl} = \frac{1}{2\pi f_{\max} R_{ct}} \quad (1)$$

Where f_{max} is the frequency at which the imaginary component of impedance is maximum. The inhibition efficiency of the inhibitor was calculated from the charge transfer resistance values using the following equation [32]:

$$\eta_z\% = \frac{R_{ct(inh)} - R_{ct}}{R_{ct(inh)}} \times 100 \quad (2)$$

Where R_{ct} and R_{ct}° represent the resistance of charge transfer in the presence and absence of inhibitor, respectively. R_{ct} is the diameter of the loop. The R_{ct} values of this investigated P2 derivative increase with increasing inhibitor concentration.

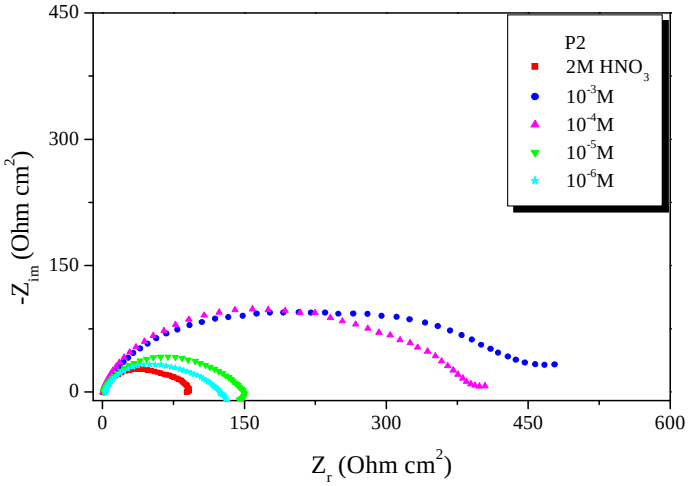

Figure 2. Nyquist diagrams for copper in 2.0 M HNO_3 containing different concentrations of P2 at 303K

Indeed, the impedance behaviour of copper in HNO_3 solutions is somewhat similar to that of copper in H_2SO_4 and HCl solutions [33]. The anodic dissolution of copper in the halide-containing solutions has been proved to be diffusion limited [34]. The diffusion step was due to the transport of CuX^{2-} to the bulk solution [35]. However, the corrosion reaction of copper in halide solutions at E_{corr} is composed of the oxidation of copper and the reduction of oxygen dissolved in the solutions [36], these two half reactions also expected to occur in aerated HNO_3 solutions. The increase in the size of the capacitive loop with the addition of P2 molecules show that a barrier gradually forms on the copper surface. The barrier is probably related to the formation of an inhibitor surface film on the electrode surface.

Table 1. Corrosion parameters obtained by impedance measurements for copper in 2.0 M HNO_3 at various concentrations of P2

Inhibitor	Conc (M)	R_{ct} (Ω cm^2)	f_{max} (Hz)	C_{dl} (μF/cm^2)	η (%)
HNO_3	2.0	091.4	15.82	110.1	-----
P2	10^{-3}	462.1	02.23	156.0	80.0
	10^{-4}	378.2	05.00	084.2	75.8
	10^{-5}	146.9	08.92	121.4	37.8
	10^{-6}	123.8	11.16	115.2	26.2

Gravimetric measurements

Effect of concentration

In the gravimetric experiment, a previously weighed metal (copper) coupon was completely immersed in 50 mL without and with different concentrations of pyridazine in an open beaker. The beaker was inserted into a water bath maintained at 303 K. From the weight loss results, the inhibition efficiency (%IE) of the inhibitor and degree of surface coverage (θ) were calculated using equations 3 and 4 [37];

$$\%IE = \left(1 - \frac{W_1}{W_2}\right) \times 100 \quad (3)$$

$$\Theta = 1 - \frac{W_1}{W_2} \quad (4)$$

Where W_1 and W_2 are the weight losses for copper in the presence and absence of the inhibitor in HNO_3 solution and θ is the degree of surface coverage of the inhibitor.

Values of corrosion rates and inhibition efficiencies are given table 2. Maximum inhibition efficiency was reported at 10^{-3} M concentration of pyridazine. It is evident from the table 2 that the corrosion rate decreases and inhibition efficiency increases with increase in P2 concentration.

Table 2. Corrosion parameters for copper in aqueous solution of 2M HNO_3 in the absence and presence of different concentrations of inhibitor from weight loss measurements at 303K

Inhibitor	Conc (M)	W (mg/cm^2 h)	IE (%)	θ
HNO_3	2	1.78	----	----
P2	1×10^{-3}	0.29	83.6	0.836
	5×10^{-4}	0.28	83.4	0.834
	1×10^{-4}	0.51	71.2	0.712
	5×10^{-5}	0.86	51.5	0.515
	1×10^{-5}	1.06	40.2	0.402
	1×10^{-6}	1.38	22.6	0.226

Adsorption isotherm and thermodynamic activation parameters

In order to study the effect of temperature on the inhibition efficiencies of P2, weight loss measurements were carried out in the temperature range 303-343K in absence and presence of inhibitor at optimum concentration. The corresponding data are shown in Table 3.

Table 3. Various corrosion parameters for copper in 2.0 M HNO_3 in absence and presence of optimum concentration of P2 at different temperatures at 1h

Temperature (K)	Inhibitor	W (mg/cm^2 h)	IE (%)	θ
303	Blank	1.78	----	----
	P2	0.29	83.6	0.836
313	Blank	7.33	----	----
	P2	1.73	76.3	0.763
323	Blank	24.97	----	----
	P2	6.06	75.7	0.757
333	Blank	70.82	----	-
	P2	26.14	63.1	0.631
343	Blank	186.61	----	----
	P2	94.43	49.4	0.494

Inspection of table 3 showed that corrosion rate increased with increasing temperature both in uninhibited and inhibited solutions while the inhibition efficiency of P2 decreased with temperature. A decrease in inhibition efficiencies with the increase temperature in presence of P2 might be due to weakening of physical adsorption.

The adsorption isotherm study that describes the adsorptive behavior of organic inhibitor is important in order to know the mechanism of corrosion inhibition. Basic information dealing with interaction between inhibitor molecules and the metal surface can be provided by adsorption isotherms. The surface coverage (θ) of different concentrations of inhibitor in acidic medium was calculated using the equation (4).

The most frequently used adsorption isotherms are Langmuir, Temkin, Frumkin and Freundluich. Several isotherms were tested. The Langmuir isotherm was found to provide the best description of the adsorption behavior. Plots C/θ versus C yield a straight line (Fig. 3) with regression coefficients, R^2, almost equal to 1.

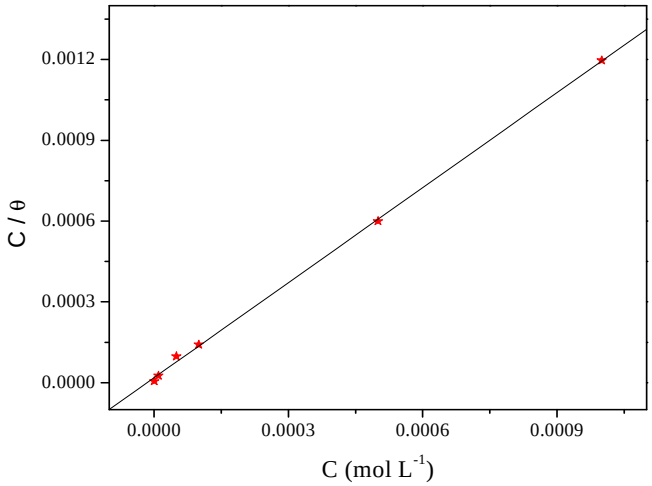

Figure 3. Langmuir adsorption isotherm for copper in 2.0 M HNO_3 containing different concentrations of copper at 303 K

This suggests that pyridazine in present study obeyed the Langmuir isotherm and there is negligible interaction between the adsorbed molecules. Free energy of adsorption was calculated using the relation:

$$\Delta G_{ads}^{\circ} = -2.303RTlog(55.55K_{ads}) \quad (5)$$

The value 55.55 is the molar concentration of water in solution [38], K_{ads} is the adsorption equilibrium constant and its value is given by

$$K_{ads} = \frac{\theta}{C(1-\theta)} \quad (6)$$

Table 4. Thermodynamic parameters for copper corrosion in 2.0 M HNO_3 in absence and presence of 10^{-3} M copper at different temperatures

Tem (K)	Free acid			P2 (10^{-3}M)				
	E_a (KJ/mol	ΔH_a (kJ/mol)	ΔS_a (J/mol K)	E_a (KJ/mol)	ΔH_a (kJ/mol)	ΔS_a (J/mol K)	K_{ads} (M^{-1})	ΔG_{ads} (kJ/mol)
303							5097.56	-31.62
313							3219.41	-31.47
323	100.21	097.53	082.36	123.57	120.89	144.26	3115.23	-32.39
333							1710.03	-31.73
343							976.28	-31.08

The free energy of adsorption calculated from relation 6 is given in Table 4. The negative value of ΔG_{ads} and the high values of the adsorption constant suggested that the adsorption of pyridazine in 2.0 M HNO_3 on the copper surface is a spontaneous process and the adsorbed layer is stable. Generally, for values of ΔG_{ads} up to -20 kJ mol^{-1}, the type of adsorption is considered as physisorption. The adsorption process is due to electrostatic interactions between the charged molecules and the charged metal [39]. The calculated ΔG_{ads} values are -31.08 to -32.39 kJ mol^{-1} indicated that adsorption mechanism of the investigated pyridazine derivative is typical of physical adsorption.

Activation parameters like activation energy (E_a), enthalpy (ΔH_a) and entropy (ΔS_a) for the dissolution of copper in 2.0 M HNO_3 in the absence and presence of 10^{-3} M pyridazine was calculated from the Arrhenius equation (Eq. (7)) and the transition state equation (Eq. (8)) [40]:

$$C_R = A\exp\left(\frac{-E_a}{RT}\right) \quad (7)$$

$$C_R = \frac{RT}{Nh}\exp\left(\frac{\Delta S_a}{R}\right)\exp\left(-\frac{\Delta H_a}{RT}\right) \quad (8)$$

Where C_R is the corrosion rate, R the gas constant, T the absolute temperature, A the pre-exponential factor, h the Plank's constant and N is Avogrado's number, E_a the activation energy for corrosion process , ΔH_a the enthalpy of activation and ΔS_a the entropy of activation. Fig. 4 showed the Arrhenius plot of Ln C_R versus 1/T which gave straight lines with slopes equal to $-E_a/R$. Again the Arrhenius plots of Ln (C_R/T) versus 1/T gave straight lines (Fig. 5) with slope ΔH_a /R and intercept (Ln R/Nh + ΔS_a /R) from which ΔH_a and ΔS_a values were calculated. The activation parameters are given in Table 4.

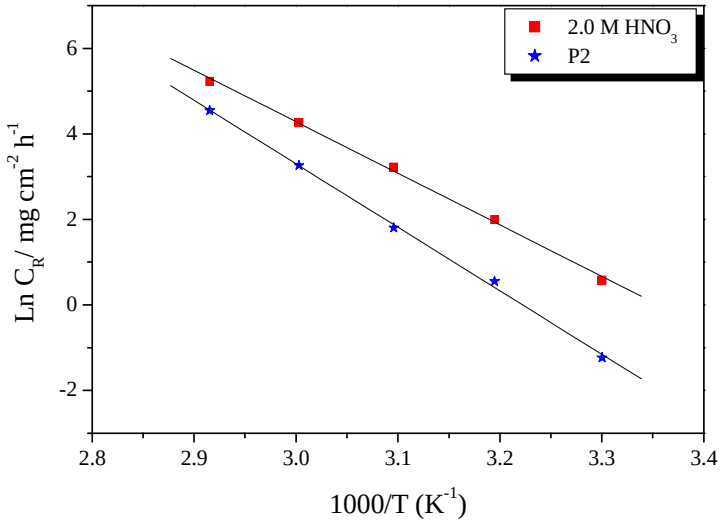

Figure 4. Arrhenius plots of log C_R vs. 1/T for copper in 2.0 M HNO_3 in the absence and the presence of pyridazine at optimum concentration

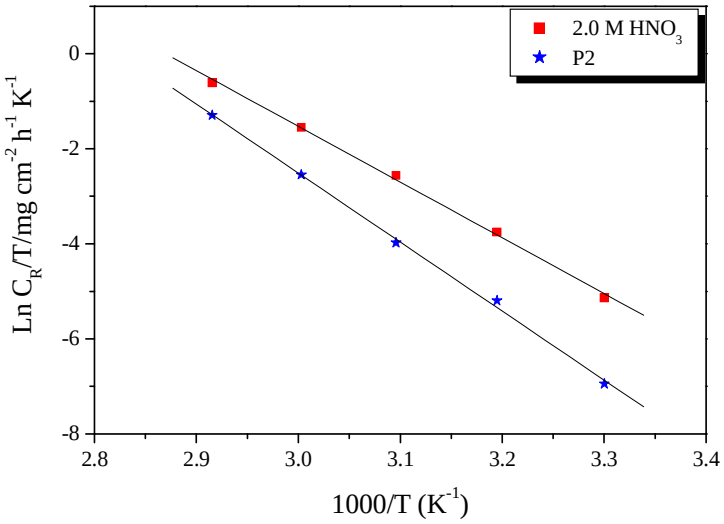

Figure 5. Arrhenius plots of log C_R/T vs. 1/T for copper in 2.0 M HNO_3 in the absence and the presence of pyridazine at optimum concentration

It was observed that the values of apparent activation energy E_a and enthalpy ΔH_a are higher in presence of inhibitor than in its absence. This indicated that the energy barrier for the corrosion reaction increases in presence of inhibitor. The value of ΔS_a is higher for inhibited solutions than that for free acid solutions. This suggested that an increase in randomness occurs on going from reactants to the activated complex. This increase in entropy of activation is attributed to the increase in solvent entropy [41].

CONCLUSION

The following conclusions can be drawn from this study:

❖ All measurements showed that the pyridazine has excellent inhibition properties for the corrosion of copper in 2.0 M HNO_3 solution. The weight loss measurements show that the inhibition efficiency decreases with increasing temperature and reaches its highest value (83.6 %) at 10^{-3} M concentration at 303K.

❖ EIS measurements also indicate that the inhibitor increases the charge transfer resistance and show that the inhibitive performance depends on adsorption of the molecules on the metal surface.

❖ The adsorption model obeys the Langmuir isotherm at 303 K. The negative values of ΔG_{ads} indicate that the adsorption of the inhibitor molecule is a spontaneous process and an adsorption mechanism is typical of physisorption.

❖ The inhibition efficiencies determined by weight loss and EIS techniques are in reasonably good agreement.

REFERENCES

[1] A. K. Singh, M. A. Quraishi, *J. Mater. Environ. Sci.,* **2010**, 1, 101.
[2] M. Prajila, J. Sam, J. Bincy, J. Abraham, *J. Mater. Environ. Sci.,* **2012**, 3, 1045.
[3] U.J. Naik, V.A. Panchal, A.S. Patel, N.K. Shah, *J. Mater. Environ. Sci.,* **2012**, 3, 935.
[4] A. Zarrouk, H. Zarrok, R. Salghi, B. Hammouti, F. Bentiss, R. Touir, M. Bouachrine, *J. Mater. Environ. Sci.,* **2013**, 4, 177.
[5] D. Ben Hmamou, R. Salghi, A. Zarrouk, H. Zarrok, S.S. Al-Deyab, O. Benali, B. Hammouti, *Int. J. Electrochem. Sci*., **2012**, 7, 8988.
[6] B. Hammouti, A. Zarrouk, S.S. Al-Deyab and I. Warad, Orient. J. Chem., 27 **(2011)** 23.
[7] A. Zarrouk, M. Messali, H. Zarrok, R. Salghi, A.A. Ali, B. Hammouti, S.S. Al-Deyab, F. Bentiss, *Int. J. Electrochem. Sci*., **2012**, 7, 6998.
[8] H. Zarrok, A. Zarrouk, R. Salghi, Y. Ramli, B. Hammouti, S. S. Al-Deyab, E. M. Essassi, H. Oudda, *Int. J. Electrochem. Sci*., **2012**, 7, 8958.
[9] A. Zarrouk, B. Hammouti, S.S. Al-Deyab, R. Salghi, H. Zarrok, C. Jama, F. Bentiss, *Int. J. Electrochem. Sci*., **2012,** 7, 5997.
[10] D. Ben Hmamou, M. R. Aouad, R. Salghi, A. Zarrouk, M. Assouag, O. Benali, M. Messali, H. Zarrok, B. Hammouti, *J. Chem. Pharm. Res*., **2012,** 4, 3489.
[11] A. Zarrouk, H. Zarrok, R. Salghi, B. Hammouti, S.S. Al-Deyab, R. Touzani, M. Bouachrine, I. Warad, T. B. Hadda, *Int. J. Electrochem. Sci*., **2012**, 7, 6353.
[12] H. Zarrok, R. Saddik, H. Oudda, B. Hammouti, A. El Midaoui, A. Zarrouk, N. Benchat, M. Ebn Touhami, *Der Pharm. Chem*., **2011**, 3, 272.
[13] A. Zarrouk, B. Hammouti, A. Dafali, H. Zarrok, *Der Pharm. Chem*., **2011**, 3, 266.
[14] A. Ghazoui, R. Saddik, N. Benchat, B. Hammouti, M. Guenbour, A. Zarrouk, M. Ramdani, *Der Pharm. Chem*., **2012**, 4, 352.
[15] D. Ben Hmamou, R. Salghi, A. Zarrouk, B. Hammouti, S.S. Al-Deyab, Lh. Bazzi, H. Zarrok, A. Chakir, L. Bammou, *Int. J. Electrochem. Sci*., **2012**, 7, 2361.
[16]A. Zarrouk, B. Hammouti, H. Zarrok, M. Bouachrine, K.F. Khaled, S.S. Al-Deyab, *Int. J. Electrochem. Sci*., **2012**, 6, 89.
[17] A. Zarrouk**,** B. Hammouti, H. Zarrok, I. Warad, M. Bouachrine, *Der Pharm. Chem*., **2011**, 3, 263.
[18] A. H. Al Hamzi, H. Zarrok, A. Zarrouk, R. Salghi, B. Hammouti, S. S. Al-Deyab, M. Bouachrine, A. Amine, F. Guenoun, *Int. J. Electrochem. Sci*., **2013**, 8, 2586.
[19] A. Ghazoui, N. Bencaht, S. S. Al-Deyab, A. Zarrouk, B. Hammouti, M. Ramdani, M. Guenbour, *Int. J. Electrochem. Sci*., **2013** 8, 2272.
[20] D. Ben Hmamou, R. Salghi, A. Zarrouk, M. Messali, H. Zarrok, M. Errami, B. Hammouti, Lh. Bazzi , A. Chakir, *Der Pharm. Chem*., **2012**, 4, 1496.
[21] A. Zarrouk, H. Zarrok, R. Salghi, N. Bouroumane, B. Hammouti, S. S. Al-Deyab, R. Touzani, *Int. J. Electrochem. Sci*., **2012**, 7, 10215.
[22] H. Bendaha, A. Zarrouk, A. Aouniti, B. Hammouti, S. El Kadiri, R. Salghi, R. Touzani, *Phys. Chem. News*, **2012**, 64, 95.

[23] J. Hmimou, A. Rochdi, R.Touir, M. Ebn Touhami, E.H. Rifi, A. El Hallaoui, A. Anouar, , D. Chebab, *J. Mater. Environ. Sci.*, **2012**, 3, 543.
[24] Y. Aouine, M. Sfaira, M. Ebn Touhami, A. Alami, , B. Hammouti, M. Elbakri, A. El Hallaoui, R. Touir, *Int. J. Electrochem. Sci*., **2012**, 7, 5400.
[25] B. Zerga, , B. Hammouti, , M. Ebn Touhami, , R. Touir, , M. Taleb, , M. Sfaira, , M. Bennajeh, , I. Forssal, , *Int. J. Electrochem. Sci*., **2012**, 7, 471.
[26] M. Cenoui, N. Dkhireche, O. Kassou, M. Ebn Touhami, R. Touir, A. Dermaj, N. Hajjaji, *J. Mater. Environ. Sci.*, **2010**, 1, 84.
[27] K. Adardour, O. Kassou, R. Touir, M. Ebn Touhami, H. ElKafsaoui, H. Benzeid, E.M. Essassi, M. Sfaira, *J. Mater. Environ. Sci.*, **2010**, 1, 129.
[28] M. ELbakri, R. Touir, M. Ebn Touhami, A. Srhiri, , M. Benmessaoud, *Corros. Sci.*, **2008**, 50, 1538.
[29] H. Ashassi-Sorkhabi, N. Ghalebsaz-Jeddi, F. Hashemzadeh, H. Jahani, *Electrochim. Acta*, **2006**, 51, 3848.
[30] R.S. Goncalves, D.S. Azambuja, A.M. Serpa Lucho, *Corros. Sci*., **2002**, 44, 467.
[31] T. Tsuru, S. Haruyama, B. Gijutsu, *J. Jpn. Soc. Corros. Eng*., **1978**, 27, 573.
[32] H. Zarrok, A. Zarrouk, B. Hammouti, R. Salghi, C. Jama, F. Bentiss, *Corros. Sci*., **2012**, 64, 243.
[33] H. Ma, S. Chen, S. Zhao, X. Liu, and D. Liu, and D. Li, *J. Electrochem. Soc*., **2001**, 148, B482.
[34] O.E. Barcia, O.R. Mattos, N. Pebere, and B. Tribollet, *J. Electrochem. Soc*., **1993**, 140, 2825.
[35] J. S. Binkley, J. A. Pople, and W. J. Hehre, *J. Am. Chem. Soc*., **1980**, 102, 939.
[36] H.P. Lee and K. Nobe, *J. Electrochem. Soc*., **1986**, 133, 2035.
[37] S. R. Lodha, *Pharmaceutical Reviews*, **2008**, 6, 1.
[38] J. Flis, T. Zarkroczymski, *J. Electrochem. Soc*., **1996**, 143, 2458.
[39] F. M. Donahue, K. Nobe, *J. Electrochem. Soc*., **1965**, 112, 886.
[40] S. S. Abd El-Rehim, M. A. M. Ibrahim, K. F. Khaled, *J. Appl. Electrochem*., **1999**, 29, 593.
[41] B. Ateya, B. El-Anadauli, F.El. Nizamy, *Corros. Sci*., **1984**, 24, 509.